

Chiral smectic-A and smectic-C phases with de Vries characteristics

Stevenson, P. (2017). Chiral smectic-A and smectic-C phases with de Vries characteristics. *Physical Review E*, 95(6), [062704]. <https://doi.org/10.1103/PhysRevE.95.062704>

Published in:
Physical Review E

Document Version:
Publisher's PDF, also known as Version of record

Queen's University Belfast - Research Portal:
[Link to publication record in Queen's University Belfast Research Portal](#)

Publisher rights
©2017 American Physical Society. This work is made available online in accordance with the publisher's policies. Please refer to any applicable terms of use of the publisher.

General rights
Copyright for the publications made accessible via the Queen's University Belfast Research Portal is retained by the author(s) and / or other copyright owners and it is a condition of accessing these publications that users recognise and abide by the legal requirements associated with these rights.

Take down policy
The Research Portal is Queen's institutional repository that provides access to Queen's research output. Every effort has been made to ensure that content in the Research Portal does not infringe any person's rights, or applicable UK laws. If you discover content in the Research Portal that you believe breaches copyright or violates any law, please contact openaccess@qub.ac.uk.

Chiral smectic-A and smectic-C phases with de Vries characteristicsNeelam Yadav,^{1,2} V. P. Panov,¹ V. Swaminathan,¹ S. P. Sreenilayam,¹ J. K. Vij,^{1,*} T. S. Perova,³ R. Dhar,² A. Panov,⁴ D. Rodriguez-Lojo,⁴ and P. J. Stevenson⁴¹*Department of Electronic and Electrical Engineering, Trinity College Dublin, University of Dublin, Dublin 2, Ireland*²*Centre of Material Sciences, University of Allahabad, Allahabad 211002, India*³*Microelectronics Group, Department of Electronic and Electrical Engineering, Trinity College, University of Dublin, Dublin 2, Ireland*⁴*School of Chemistry & Chemical Engineering, Queens University, Belfast BT7 1NN, United Kingdom*

(Received 23 February 2017; revised manuscript received 23 April 2017; published 21 June 2017)

Infrared and dielectric spectroscopic techniques are used to investigate the characteristics of two chiral smectics, namely, 1,1,3,3,5,5,5-heptamethyltrisiloxane 1-[4'-(undecyl-1-oxy)-4-biphenyl(S,S)-2-chloro-3-methylpentanoate] (MSi₃MR₁₁) and tricarbosilane-hexyloxy-benzoic acid (S)-4'-(1-methyl-hexyloxy)-3'-nitro-biphenyl-4-yl ester (W599). The orientational features and the field dependencies of the apparent tilt angle and the dichroic ratio for homogeneous planar-aligned samples were calculated from the absorbance profiles obtained at different temperatures especially in the smectic-A* phase of these liquid crystals. The dichroic ratios of the C-C phenyl ring stretching vibrations were considered for the determination of the tilt angle at different temperatures and different voltages. The low values of the order parameter obtained with and without an electric field applied across the cell in the Sm-A* phase for both smectics are consistent with the de Vries concept. The generalized Langevin-Debye model introduced in the literature for explaining the electro-optical response has been applied to the results from infrared spectroscopy. The results show that the dipole moment of the tilt-correlated domain diverges as the transition temperature from Sm-A* to Sm-C* is approached. The Debye-Langevin model is found to be extremely effective in confirming some of the conclusions of the de Vries chiral smectics and gives additional results on the order parameter and the dichroic ratio as a function of the field across the cell. Dielectric spectroscopy finds large dipolar fluctuations in the Sm-A* phase for both compounds and again these confirm their de Vries behavior.

DOI: [10.1103/PhysRevE.95.062704](https://doi.org/10.1103/PhysRevE.95.062704)**I. INTRODUCTION**

For successful applications of liquid crystals in devices, chiral smectics can play an important role since they possess numerous desirable characteristics over nematics. The chiral smectics in particular when sandwiched in cells have much higher operational speeds due to the interaction of the electric field with the spontaneous polarization as opposed to a relatively weak interaction with the dielectric anisotropy in nematics [1]. The spontaneous polarization arises from the lack of the mirror symmetry (due to chirality) in a plane at right angles to the twofold symmetry axis. The polarization is parallel to this twofold axis and its direction dependent on the applied electric field. The chirality also gives rise to a helical structure with the helical axis being parallel to the layer normal. The helix is unwound by the electric field applied along the twofold axis or by the surface interactions of molecules. In the smectic phases, the rod-shaped molecules exhibit positional order at least in one dimension apart from the orientational order defined by de Gennes [2] in terms of a complex order parameter $\Phi e^{i\alpha}$. This quasi-one-dimensional translational order is a result of the Landau-Peierls instability theorem [2] which states that the mean squared displacement of the smectic layers diverges logarithmically from their equilibrium position due to thermal fluctuations. The uniaxial smectic-A (Sm-A) phase has an average orientation of the long molecular axes defined by the director \vec{n} , which coincides with the perpendicular drawn to the smectic layers, while in the biaxial smectic-C (Sm-C) phase,

the director \vec{n} is tilted by an angle dependent on temperature with respect to the layer normal. If these molecules are chiral, then chiral phases denoted by (*) are formed. In the Sm-A* phase, an electro-optical effect (known as the electroclinic effect) was first observed by Garoff and Meyer [3]. A uniform molecular tilt is induced in a plane perpendicular to the applied electric field E . This plane coincides with the substrate's plane for a planar-aligned cell, formed by the layer normal and the projection of the tilted director onto this plane. The electroclinic effect can be explained by a model deduced from the Landau theory which predicts linearity between E and the induced tilt at low electric fields. But the linear behavior deviates as the temperature approaches the orthogonal Sm-A* to tilted Sm-C* transition. This effect is accompanied by the contraction of the smectic layers in magnitude by as large as 13% [4] scaled by the cosine of the tilt angle, resulting in their buckling into first vertical and then horizontal chevron structures [5]. These are visible as periodic stripe domains viewed under the crossed polarizers of a microscope. The chevron structure leads to the appearance of the zigzag defects in the cell. The striped domain textures and the zigzag defects do adversely affect the contrast ratio, acting as roadblocks to the commercialization of smectics in devices.

The impetus to overcome the above problems in smectics led to finding materials with minimal layer shrinkage in their tilted phases. De Vries had reported a material which showed only 1% layer contraction [6] deep in its Sm-C phase and had explained this feature by the noncorrelation model which assumed that stacks of smectic layers are formed in the Sm-A phase with molecules tilted permanently and uniformly in each layer [7]. The experimental x-ray scattering results obtained

*Corresponding author: jvij@tcd.ie

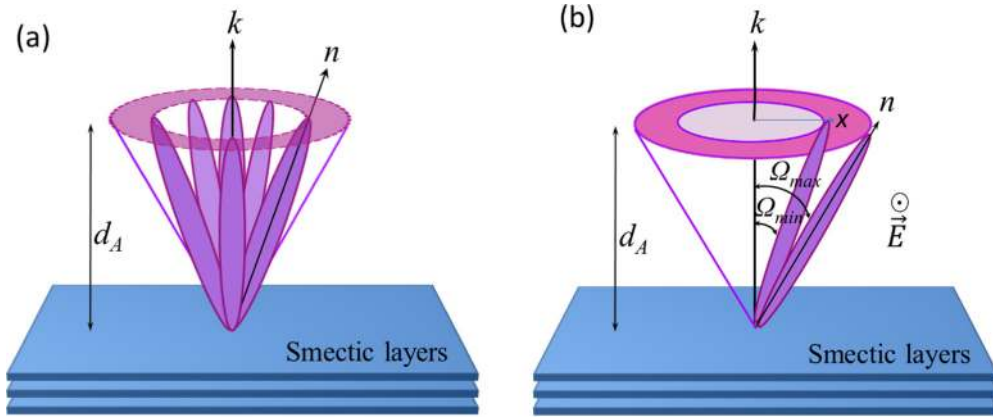


FIG. 1. Schematic illustration of the de Vries diffuse-cone model in the Sm-A* phase. Here \vec{k} is the layer normal, \vec{n} is the direction of long molecular axis, d_A is the layer spacing, while Ω_{\max} is the maximum tilt angle at a large field, and Ω_{\min} is evaluated from the experimental data on birefringence at zero field. The azimuthal angle is distributed on the cone at zero field. The apparent tilt angle is thus zero. For higher fields, the azimuthal angle condenses to an almost single value leading to the maximum apparent angle, Ω_{\max} . The apparent tilt angle Ω_0 varies with the field.

by de Vries and those of Leadbetter and Norris on some new smectic liquid crystals [8] revealed that (a) the layer thickness in the Sm-A phase is much lower than the molecular length and (b) the order parameter observed in the Sm-A phase is much lower than unity. In order to explain these results de Vries proposed a diffuse-cone model for the Sm-A phase in which the azimuthal angle of the molecular directors is distributed onto a cone; the axis of the cone is directed along the layer normal with a finite cone angle [9]. In the Sm-C* phase, however, the azimuthal degeneracy in a layer is lifted as the molecules are azimuthally ordered in a particular direction without affecting the magnitude of the polar tilt angle. Due to the molecular chirality, the azimuthal angles in Sm-C* vary systematically from layer to layer to form a macroscopic helical structure. The azimuthal redistribution of directors takes place when an electric field is applied across a planar-aligned cell in this phase. Some of the antiferroelectric liquid crystals that have been investigated show characteristics of de Vries smectics [10,11].

Figure 1 depicts the schematic representation of the diffuse-cone model in the Sm-A* phase. Some of the materials in Sm-A* called “de Vries smectics” are known to exhibit a large electroclinic effect, a large increase in the birefringence with the field, and a minimal layer shrinkage at the Sm-A* to Sm-C* transition as well as in the Sm-C* phase [4]. In recent years a large number of such Mesogens have been synthesized [12,13], with siloxane or perfluorinated segments at the end of side chains (both of which are known to promote increased lamellar order), that exhibit low orientational order due to nanosegregation of the constituents.

In addition to the above model, other alternate models have been suggested in the literature for de Vries smectics. The conformational change model, also known as the zigzag model [14], assumes that the mesogens with tilted side chains and upright cores form a kinked conformation structure. The cluster diffuse-cone model based on the results obtained from nuclear magnetic resonance spectroscopy considers the presence of tilted molecules in clusters. These are useful in explaining the magnetoclinic effect [15]. The interdigitation

model proposed by some authors [16,17] states that the mesogens are interdigitated and this leads to low values of the orientational order parameter. The sugar-loaf model based on the Maier-Saupe orientational distribution function is predicted to be in close agreement with the experimental x-ray scattering results on de Vries smectics [18].

In this article, we report the infrared and dielectric studies carried out on two de Vries smectics in order to advance the understanding of de-Vries-ness especially in the Sm-A* phase, which is not fully understood as yet. At present, a number of theoretical models are being tested for explaining an entire gamut of the experimental results. Additional testing of these models using data acquired by other techniques such as IR spectroscopy is timely and important. The two techniques of polarized IR and dielectric spectroscopy are proven to have yielded new results for the orientational order parameter and the tilt angle as a function of the bias field. The polarized infrared (IR) technique provides a direct measurement of the dichroic ratio and the order parameters of the liquid crystal (LC) molecules as a function of the field rather easily which may not be the case with other techniques.

II. EXPERIMENTAL SECTION

A. Materials

The chemical formulae of the two compounds, 1,1,3,3,5,5,5-heptamethyltrisiloxane 1-[4'-(undecyl-1-oxy)-4-biphenyl(S,S)-2-chloro-3-methylpentanoate] (MSi₃MR₁₁) [19] and tricarbosilane-hexyloxy-benzoic acid (S)-4'-(1-methyl-hexyloxy)-3'-nitro-biphenyl-4-yl ester (W599) [27], their phase sequences, and their transition temperatures are given in Fig. 2. These compounds were resynthesized by the Stevenson group in Belfast; the synthesis of MSi₃MR₁₁ in particular is described in [26]. MSi₃MR₁₁ is made up of a biphenyl 2-chloro-3-methylpentanoate core with a trisiloxane backbone while W599 has a tricarbosilane tail. The carbosilane tail can restrain the out-of-layer fluctuations and thus can lead to the formation of a better bookshelf smectic layer structure in the Sm-A* phase.

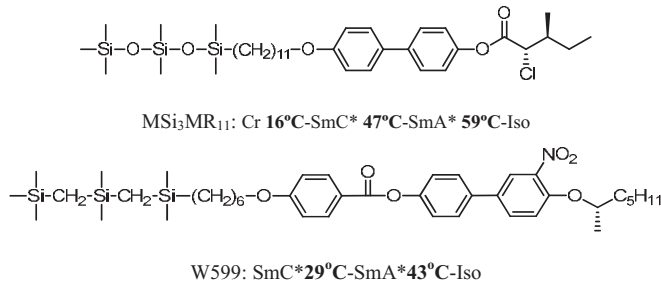


FIG. 2. The molecular structures of $\text{MSi}_3\text{MR}_{11}$ (top) and W599 (bottom) with their corresponding phase transition temperatures ($\text{MSi}_3\text{MR}_{11}$: Cr 16°C, Sm-C* 47°C, Sm-A* 59°C, Iso; W599: Sm-C* 29°C, Sm-A* 43°C, Iso) obtained by polarized optical microscopy at a cooling rate of 1°C/min are specified.

B. Measurements

The polarized IR measurements were performed on $\text{MSi}_3\text{MR}_{11}$ and W599 compounds, using a Bio-Rad FTS-6000 spectrometer in the 450 to 4000 cm^{-1} wave number range. The spectrometer is equipped with a liquid nitrogen cooled mercury cadmium telluride (MCT) detector, a computer-controlled wire grid rotation polarizer, and a hot stage where a temperature stability to within $\pm 0.1^\circ\text{C}$ can be attained for these investigations. A total of 64 experimental scans are averaged to make the signal-to-noise ratio get above 2000 for a 2 cm^{-1} spectral resolution. The homogeneous planar alignment of LC molecules is achieved as follows: two zinc selenide (ZnSe) windows covered with a thin layer of indium tin oxide (ITO) are used to make a sandwich-type LC cell. The Mylar spacers of 5 μm thickness are used to separate these two overlapping windows. Both windows are coated with a polymer solution RN1175 (Nissan Chemicals), following which the windows are kept in an oven at 250°C for one hour. The windows are rubbed and rubbing directions are antiparallel to each other. The IR spectra are recorded in both Sm-A* and Sm-C* phases with a greater emphasis laid on the detailed measurements being carried out in the former. The dc bias voltages of both polarities (positive and negative) are applied to cells. The polarizer is rotated from an angle of 0° to 180° in steps of 10° for each applied voltage. For each of its positions, the IR spectra are recorded. The Perkin-Elmer GRAMS Research (PEGR) program is used to analyze the intensity and the width of each measured spectral line while the Origin 7.5 program is used to fit each absorbance profile. Dielectric measurements are carried out using a Novocontrol impedance analyzer in the frequency range of 0.1 Hz to 10 MHz with an alternating rms voltage of 0.1 V applied across the cell. For dielectric experiments, ITO-coated glass substrates are used and treated in the same way as were the ZnSe windows, to order to obtain the planar alignment of the LC molecules. The sheet resistance of the ITO-coated glass substrate, R , is $\sim 30 \Omega/\square$, rather high. This resistance is in series with the cell capacitance, C . The time constant of the combination, RC , should normally shift the peak frequency, $f = 1/(2\pi RC)$, of this parasitic RC arrangement beyond 1 MHz (highest frequency in the experimental window). The experimental results of the measurements should ideally be free from the ITO parasitic effect.

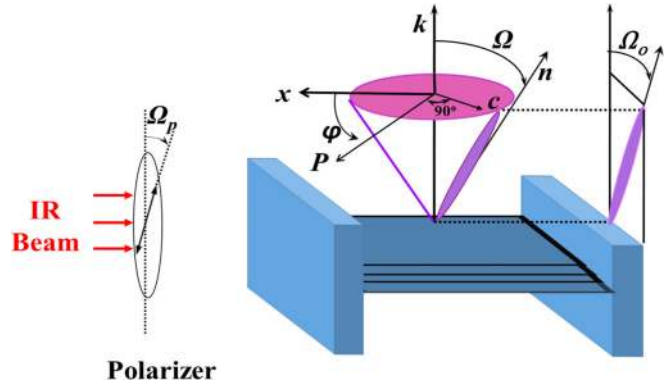


FIG. 3. A schematic representation of the measurement system for the de Vries Sm-A* phase. ZnSe windows coated with ITO containing the sample are mounted on the hot stage. The polarizer can be automatically rotated by an angle Ω_p . The constituent molecules are tilted by Ω from the layer normal \hat{k} . The polarization P that is normal to the c director (projection of the molecular director on the smectic plane) makes an angle φ with the normal drawn to the cell, while Ω_o is the angle between the layer normal and the projection of the effective optic axis onto the plane of the cell's windows.

III. RESULTS AND DISCUSSION

A. Polarized IR spectroscopy

The infrared studies are performed on cells with ITO-coated ZnSe windows as illustrated in Fig. 3. The infrared spectra of the sample cell consist of several absorption bands; these pertain to the different molecular groups of the constituent molecules of the system. From these spectra, the C-C phenyl ring stretching vibration is chosen to carry out a detailed analysis of the LC system since the transition dipole moment of these vibrations, positioned at 1608 cm^{-1} for $\text{MSi}_3\text{MR}_{11}$ and 1605 cm^{-1} for W599, is approximately parallel to the long molecular axis in each of these compounds. The absorbance profile $A(\Omega)$ for this C-C band is a function of the angle by which the polarizer is rotated under the application of negative and positive dc voltages across a planar-aligned cell. The experimental data as a polar plot of A vs Ω_p are presented in Figs. 4(a) and 4(b), for different values of the applied dc voltage. A unique absorbance profile is constructed for each applied voltage and is fitted to the equation [20–22]

$$A(\Omega_p) = -\log_{10}[10^{-A_{\parallel}} + (10^{-A_{\perp}} - 10^{-A_{\parallel}})\sin^2(\Omega_p - \Omega_o)], \quad (1)$$

where the polarizer angle is denoted by Ω_p , minimum and maximum values of the absorbance at different polarizer angles $[A(\Omega_p)]$ are given by A_{\perp} and A_{\parallel} , while the polarizer angle at which absorbance for the phenyl stretching vibration is maximum is represented by Ω_o (the apparent tilt angle). The dichroic ratio R (from now on) is defined as A_{\parallel}/A_{\perp} while the orientational order parameter S is calculated using the equation derived in Ref. [23],

$$S = \frac{R - 1}{R + 2}. \quad (2)$$

The tilt angle R , A_{\perp} and A_{\parallel} , and S for the phenyl band are plotted as a function of the electric field for both

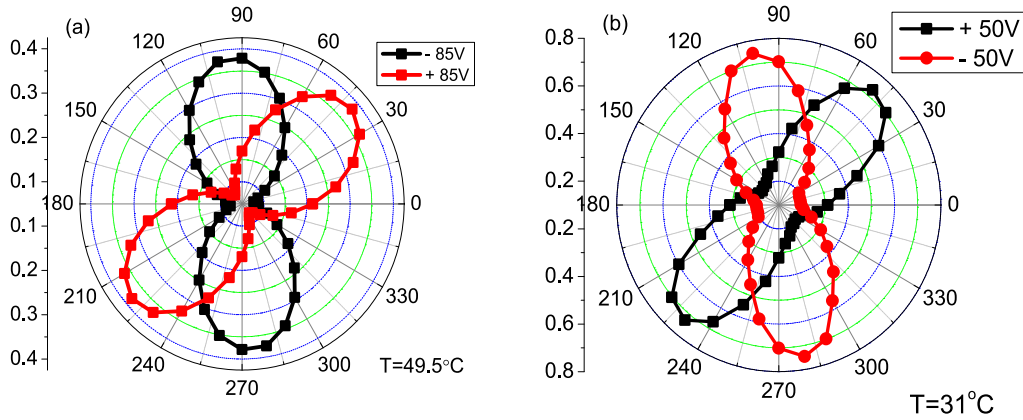


FIG. 4. Polar plots of the absorbance profiles for the C-C phenyl ring stretching vibrational band for both negative and positive fields at temperatures of (a) 49.5 °C for MSi₃MR₁₁ and (b) 31 °C for W599. These temperatures correspond to the Sm-A* phase of these materials at zero field.

MSi₃MR₁₁ and W599 in Figs. 5–9. The dependencies of the above parameters on the applied field for various temperatures is intriguing. In the Sm-A* at 52.5 °C for MSi₃MR₁₁ and 34 °C for W599, with an increase in the applied voltage (field = voltage/cell thickness), the tilt angle shows a linear behavior which is due to the electroclinic effect. The shape of the curves starts changing as the LC cell approaches the transition temperature from the Sm-A* to Sm-C* phase.

The dependence of the tilt angle, the dichroic ratio R , and the order parameter S show nonlinearity and eventual saturation, with applied voltage close to the Sm-A* to Sm-C* transition temperature. A sigmoidal-type response is seen close to this transition temperature. In the Sm-C* phase, the tilt angle, the ratio R , and the order parameter S increase rapidly with voltage but are saturated at relatively low voltages. An unwinding of the helical structure leads to a large increase in R for both compounds studied here. This increment can be attributed to a decrease in A_{\perp} and increase in A_{\parallel} (see Figs. 7 and 8). Minimum absorbance (A_{\perp}) is proportional to the average value of the squares of the projections of transition dipole moments of the phenyl ring in a direction perpendicular to the directors in the tilt plane. The direction of the tilt angle (Ω_o) starts moving to the direction of the molecular tilt and with the unwinding of the helix leads to a decrease in A_{\perp} and a consequent increase in R . This is quite contrary to the normal Sm-A* to Sm-C* transition where the values of R and S especially in the Sm-A* do not depend on voltage and stay almost constant with field [24]. A simple simulation was performed using Maple software to elucidate our experimental results. The value of R should be less in the de Vries phase than in the unwound state when no voltage is applied to it. R can be calculated from the absorbance profile obtained in the unwound state and integrating it over ψ so that a fictitious distribution of molecular tilt directions is introduced according to the equation given below [25]:

$$A(\Omega_p) = \frac{1}{2\pi} \int_0^{2\pi} -\log_{10} \left(10^{-A_{\parallel}} + (10^{-A_{\perp}} - 10^{-A_{\parallel}}) \sin^2 \right. \\ \left. \times \left\{ [\Omega_p - \Omega_o \times \cos(\psi)] \frac{\pi}{180} \right\} \right) d\psi. \quad (3)$$

On inserting the experimental parameters A_{\perp} and A_{\parallel} , R , and Ω_o obtained for the unwound state in the above equation, the dichroic ratio at the various temperatures in the Sm-C* and Sm-A* phases for the random undisturbed state is calculated. Since the helical pitch of the samples is less than the aperture of the infrared beam passing through them, Eq. (3) is applicable for both phases. The value of R in the undisturbed state comes out to be 3.2 for MSi₃MR₁₁ at 50.5 °C and 2.8 for W599 at 31 °C. The results obtained are in accordance with the experimental values. R is found equal to 4 for MSi₃MR₁₁ and 3.5 for W599 in the Sm-C* phase. For the Sm-C* phase, the simulated values slightly deviate from those of experiments. A plausible explanation for the discrepancy between the two is as follows: surfaces in a planar-aligned cell tend to distort the helical structure of the Sm-C* phase.

Values of the tilt angle with the applied voltage obtained by us show striking similarities in magnitude and response to the tilt angles measured by the electro-optical method [26,27] for both samples. For W599, Shen *et al.* [27] found the tilt angle saturated at an angle as large as $\sim 33^\circ$ [27]; they applied higher electric fields up to 35 V/ μm , while in our case the maximum field applied was 10 V/ μm resulting in a lower tilt angle, fully saturated at 28° . It has also been proven in the literature that both W599 and MSi₃MR₁₁ are de Vries smectics and they satisfy the criterion of the lower layer shrinkages of 0.73% and 1.75% at 10 °C and 20 °C, respectively, below the Sm-A* to Sm-C* transition temperature. The orientational order parameters for both materials are found to be low under zero electric field. The order parameter increases with the field, consistent with the de Vries scenario. In the Sm-A* phase, azimuthal angles of the molecular directors of calamitic mesogens are disordered. It is natural that for a disordered arrangement, the orientational order parameter is low for a wider distribution of the director orientations, whereas on the application of an electric field in the Sm-C* phase, the azimuths get aligned in a particular direction and sense. While the layer spacing remains almost constant, the average local directors tilt with respect to the layer normal. Hence the measured orientational ordering of the molecular directors in the Sm-C* phase along the optical axis is higher than in the Sm-A* phase.

B. Recent models of de Vries smectics

Several theoretical models have been suggested to explain the unusual electro-optical response of de Vries smectics, the first being that of the Langevin-Debye model that had originally been proposed by Fukuda [28] to explain the thresholdless switching in tilted chiral smectics. This model was used by Clark *et al.* [29] to explain the electro-optical properties of de Vries materials C4 and C6. This model assumes that in the absence of an electric field in the Sm-A* phase at a fixed temperature, the molecules are tilted with a fixed tilt angle and are azimuthally distributed randomly on a cone so that $\langle \cos \varphi \rangle = 0$. When the electric field E is applied, E is coupled to the polarization. The resulting free energy equals $U = -pE \cos \varphi$, where p is the local dipole moment. But the model though partly successful has failed

to explain the correct shape of the curves for apparent tilt angle versus E for temperatures closer to the Sm-A* to Sm-C* transition. In 2013 Shen *et al.* introduced a modification to this model and it is now called the generalized Langevin-Debye model [27]. This considers the orientational distribution with a complete azimuthal degree of freedom. In addition, the tilt angle can change with applied E only within a range of values. The free energy has a quadratic term scaled by a phenomenological parameter α . This is especially introduced to explain the sigmoidal response of Ω_o vs E . The free energy is expressed as $U = -p_0 E \sin \Omega \cos \varphi - \alpha p_0 E^2 \sin \Omega \cos^2 \varphi$, where $p = p_0 \sin \Omega$ is the dipole moment of the tilt-correlated domain.

The apparent electro-optical tilt angle is given by

$$\tan 2\Omega_o = \frac{\langle \sin 2\Omega \cos \varphi \rangle}{\langle \cos^2 \Omega - \sin^2 \Omega \cos^2 \varphi \rangle}. \quad (4)$$

An average $\langle X \rangle$ is written as $\langle X \rangle = \int_{\Omega_{\min}}^{\Omega_{\max}} \int_0^{2\pi} X(\Omega, \varphi) f(\Omega, \varphi) \sin \Omega \, d\Omega d\varphi$, where the mean

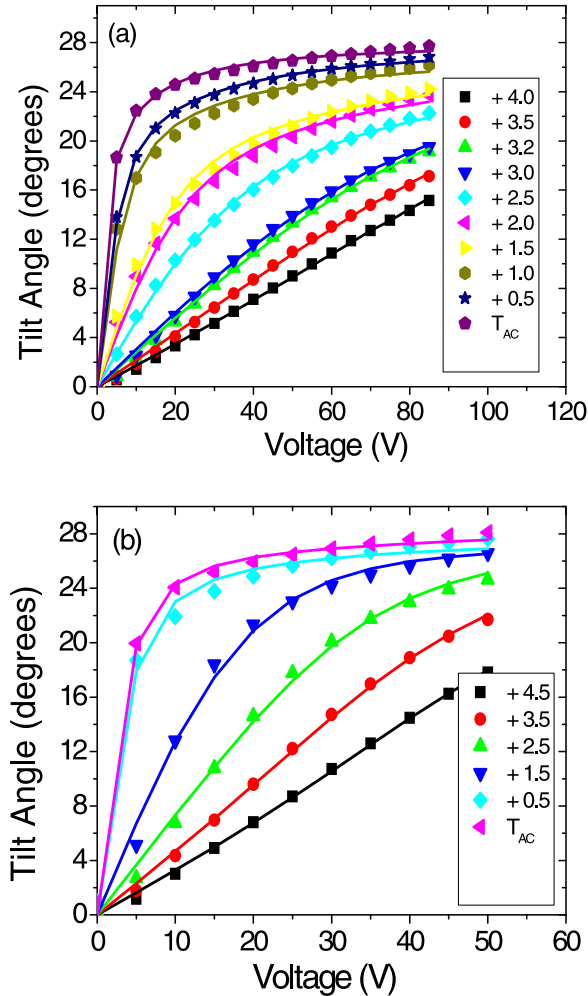


FIG. 5. Voltage dependence of the molecular tilt angle (Ω_o), determined from the absorbance profiles of the C-C phenyl ring stretching vibration at various temperatures in the Sm-A* phase but close to the Sm-A* to Sm-C* transition for (a) MSi₃MR₁₁ at 1608 cm⁻¹ and (b) W599 at 1605 cm⁻¹. The symbols correspond to the experimental data, while the solid lines are fits to the generalized Langevin-Debye model given in Sec. III B. The thickness of the sample is 5 μ m. (+) Temperatures in the inset denote above the transition temperature T_{AC} in the Sm-A* phase.

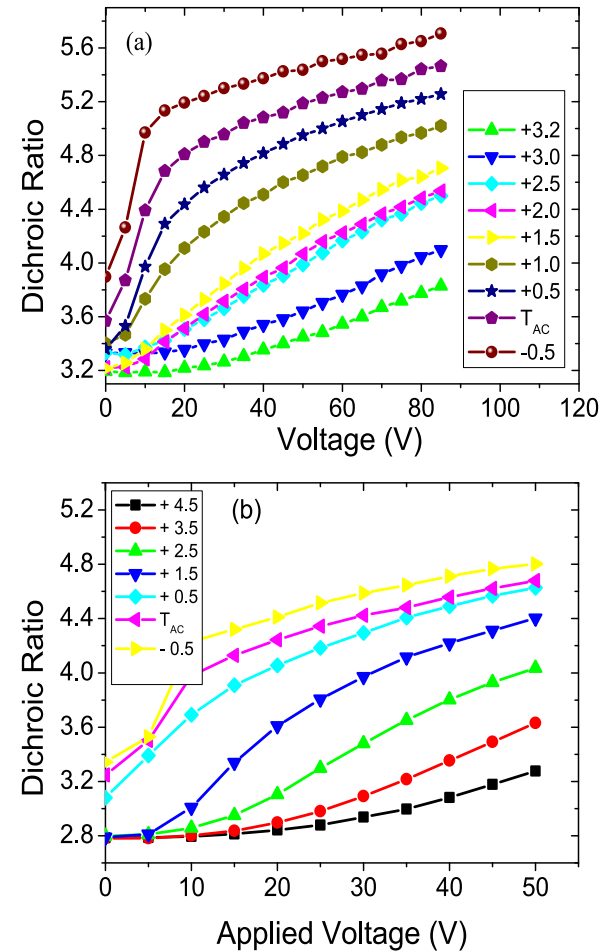


FIG. 6. Dichroic ratio ($R = A_{\parallel}/A_{\perp}$) versus the applied dc voltage for the phenyl band 1608 cm⁻¹ at different temperatures for a homogeneous planar-aligned cell of 5 μ m thickness for (a) MSi₃MR₁₁ and (b) W599. (+) Temperatures in the inset denote above T_{AC} transition temperature in the Sm-A* phase and (-) denote below it in the Sm-C* phase.

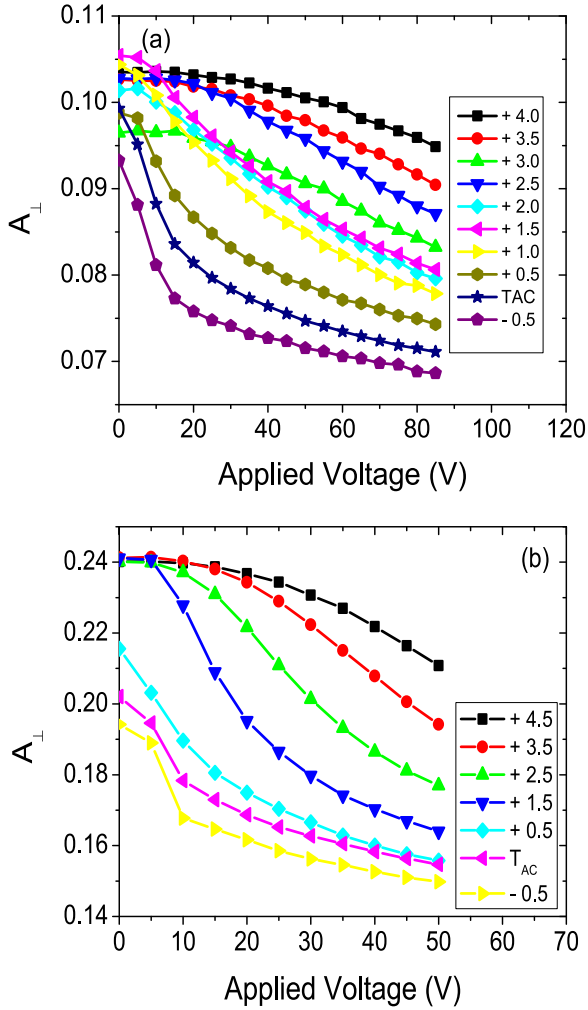


FIG. 7. Variation of A_{\perp} with voltage for a homogeneous planar-aligned cell of $5 \mu\text{m}$ thickness. (a) $\text{MSi}_3\text{MR}_{11}$ and (b) W599.

field orientation distribution is given by [25]

$$f(\Omega, \varphi) = \exp[-U/k_B T] / \int_{\Omega_{\min}}^{\Omega_{\max}} \int_0^{2\pi} \exp[-U/k_B T] \sin \Omega d\Omega d\varphi.$$

This formalism is used here to fit the tilt angle obtained from the infrared measurements of $\text{MSi}_3\text{MR}_{11}$ and W599. The angle in the lower limit Ω_{\min} is extracted from the experimental birefringence measurements made in the absence of the electric field applied to the cell. The birefringence data are taken from the literature [26,27]. It can be observed from Figs. 5(a) and 5(b) that the experimental data fits to the model quite well. The maximum tilt angle saturated at high fields (Ω_{\max}) is 28.4° for $\text{MSi}_3\text{MR}_{11}$ and 28.6° for W599. The fitting parameter p_0 , called the local dipole moment (see Fig. 10), increases on cooling from the Sm-A* phase close to the Sm-A* to Sm-C* transition. As the temperature approaches the transition temperature, p_0 diverges as the azimuthal angle condenses to values first restricted within a limited range and then it finally condenses to a single value. For W599, values of p_0 are similar in magnitude to those obtained in Ref. [27] at temperatures well above the Sm-A* to Sm-C* transition

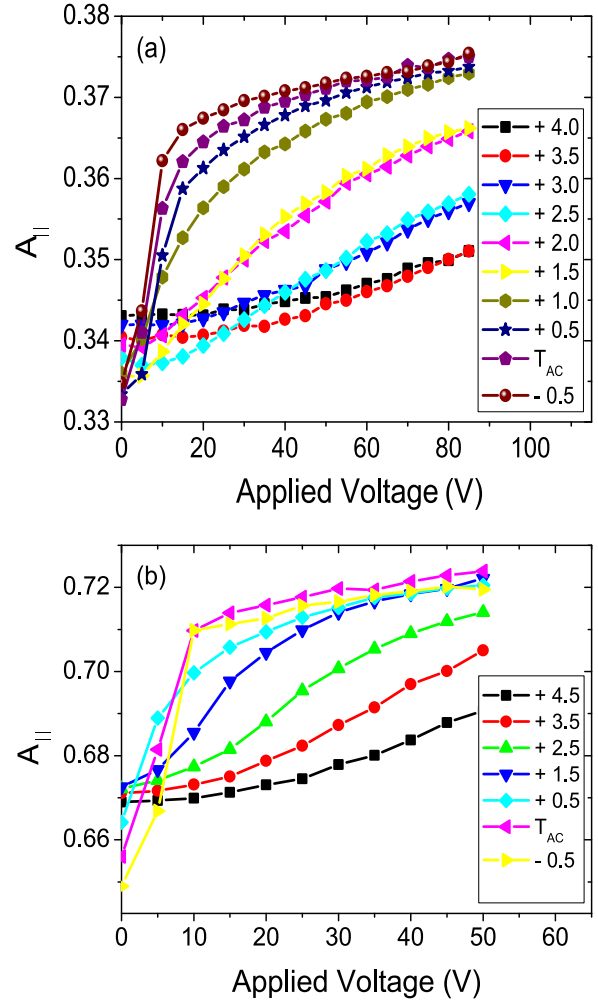


FIG. 8. Voltage dependence of A_{\parallel} at different temperatures for (a) $\text{MSi}_3\text{MR}_{11}$ and (b) W599 for a homogeneous planar-aligned cell of $5 \mu\text{m}$ thickness. (+) and (−) temperatures in the insets as in Figures 5 and 6.

temperature. But p_0 increases to higher values of the order of 10^3 at temperatures closer to the Sm-A* to Sm-C* transition temperature. Such large values of the local dipole moment were previously reported by Selinger *et al.* for TSiKN65 and DSiKN65 [30].

Another model called the generalized 3D X-Y model [31] has recently been introduced. This gave an explanation for the first-order Sm-A* to Sm-C* transition and of the sigmoidal response observed for $\text{MSi}_3\text{MR}_{11}$ and W599. Using Monte Carlo simulations they demonstrated that polarization as a function of the electric field follows the sigmoidal response for a liquid crystal compound W530 and this feature is attributed to the steric interactions inbuilt in a hollow cone of the de Vries smectic – A* phase.

The model suggested by Zappitelli *et al.* [32] considers both bulk and surface electroclinic effects in the Sm-A* phase and analyzes the tilt-dependent layer spacing and the effect of applied electric field on the layer spacing for de Vries smectics exhibiting the first-order Sm-A* to Sm-C* transition. These have a low orientational order parameter in agreement with our experimental findings. The order parameter with and

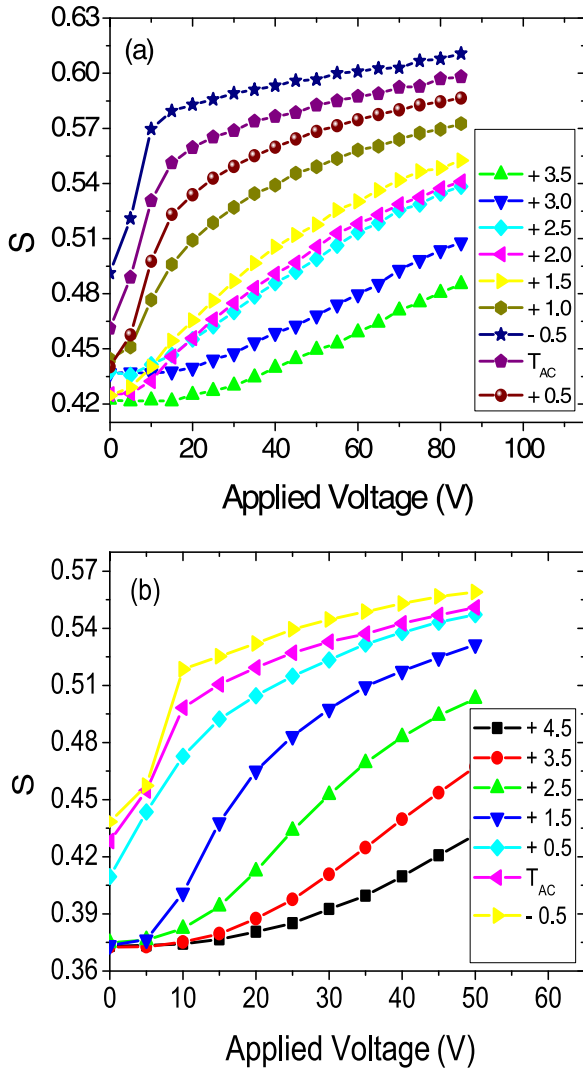


FIG. 9. Dependence of S on applied voltage for a homogeneous planar-aligned cell of $5 \mu\text{m}$ thickness. (a) $\text{MSi}_3\text{MR}_{11}$ and (b) W599. (+) and (−) in the inset imply the same as in Figs. 6 to 8.

without electric field for both smectic phases shown in Fig. 9 is lower than for the conventional smectics. Such low values of the order parameter were previously observed by Collings *et al.* [33] for TSiKN65 and DSiKN65 with dyes dissolved in them. They attributed these low order parameters to the segregation of siloxane segments within each layer. Hayashi *et al.* [34] using Raman spectroscopy found a low order

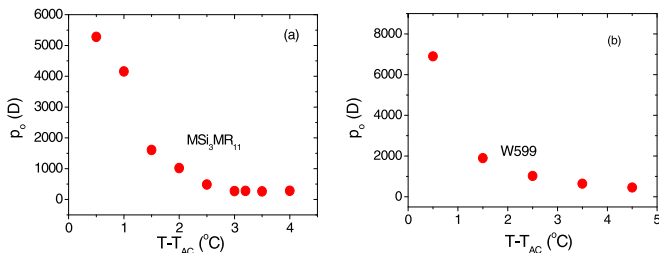


FIG. 10. The local dipole moment p_0 obtained from the fitting of the experimental data to the model as a function of the reduced temperature in the Sm-A^* phase.

parameter for TSiKN65 both with and without field. They attributed this to a large tilt ($\sim 30^\circ$) of the mesogen (treated as a rigid core) from the long molecular axis.

C. Electro-optic response in Sm-A^* phase

The electroclinic (EO) response arising from the tilt of the mesogen induced by a weak field (sinusoidal signal of amplitude 0.4 V at frequency of 22 Hz applied across a homogeneous planar-aligned cell of thickness $4 \mu\text{m}$) has been measured. The planar-aligned liquid crystal cell is mounted in a hot stage. The latter is fixed to the rotating stage of a polarizing microscope with crossed polarizer and analyzer. In the absence of the electric field, the transmitted intensity I is given by [35]

$$I = I_0 \sin^2(2\alpha) \sin^2\left(\frac{\pi \Delta n d}{\lambda}\right). \quad (5)$$

I_0 is the incident intensity, α is the angle between the optical axis of the cell and the polarizer, and α is fixed at 22.5° in order to get a maximum change in the intensity of the transmitted light due to a change in α with field. Δn is the birefringence, d is the thickness of the sample cell, and λ is the wavelength of the incident light. When a weak electric field is applied across the cell, a change in the intensity of the transmitted light with angle induced by the field, $d\alpha = \theta_{\text{ind}}$, results in differentiating Eq. (5) with respect to α ,

$$\delta I = 4I_0 \sin 4\alpha d\alpha \sin^2\left(\frac{\pi \Delta n d}{\lambda}\right). \quad (6)$$

On dividing Eq. (6) by Eq. (5), substituting $\alpha = 22.5^\circ$, and having $\theta_{\text{ind}} = d\alpha$, we obtain

$$\theta_{\text{ind}} = \frac{\delta I}{4I}. \quad (7)$$

θ_{ind} is proportional to the first harmonic EO signal. I is the dc component of the signal. The electro-optic response given by $\delta I/4I$ is proportional to θ_{ind} . The latter is linearly related to the field in the low-field approximation. The curve so obtained can be fitted to the power-law equation as

$$\text{EO response} = \frac{B}{(T - T_C)^\gamma}. \quad (8)$$

B is the scaling factor, T_C is temperature of the Sm-A^* to Sm-C^* transition, and γ is the power-law exponent that expresses the magnitude of EO response with temperature for temperatures closer to the Sm-A^* to Sm-C^* transition. Figure 11 represents the temperature-dependent electro-optical response of W599. The magnitude of γ is found to be 1.59, which lies in between 1.4 to 2, appropriate for the de Vries smectics that exhibit short-range correlations in a smectic layer as well as across the smectic layers and display a weak first-order Sm-A^* to Sm-C^* transition. The short-range correlation in de Vries smectics extends from 2 to 3 dimensions as opposed to a conventional two-dimensional ($\gamma = 1.32$) fluid as smectic [36].

D. Dielectric spectroscopy

The dielectric loss peak of W599 in a planar-aligned cell in Sm-A^* is (see Fig. 12) identified as due to the soft mode (SM). This arises from the softening of fluctuations in the tilt. The

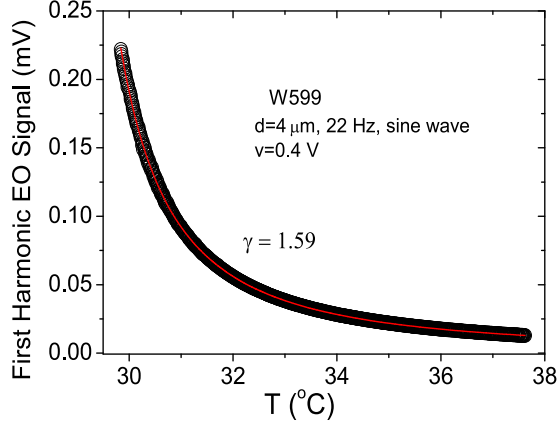


FIG. 11. Electro-optical response of W599 as a function of temperature in the Sm-A* phase.

response in the Sm-C* is due mainly to the Goldstone mode (GM); the azimuthal reorientation on the cone is seen in the low-frequency region (see Fig. 12). The dielectric relaxation frequency and dielectric strength are obtained by fitting the complex permittivity plots to the Havriliak-Negami equation using the WINFIT software purchased from Novocontrol GmbH. Since only a single mode is dominant in each phase, the Havriliak-Negami equation is used for a single mode of relaxation [37]:

$$\varepsilon^*(\omega) = \varepsilon_\infty + \frac{\Delta\varepsilon}{[1 + (i\omega\tau)^\alpha]^\beta} - \frac{i\sigma_{dc}}{\varepsilon_0\omega}. \quad (9)$$

Here ε_∞ is the high-frequency permittivity depending on the atomic and electronic polarizability, $\omega = 2\pi f$ is the angular frequency, ε_0 is the permittivity of free space, $\Delta\varepsilon$ refers to the dielectric relaxation strength, and α ($0 \ll \alpha \leq 1$) and β ($0 \ll \beta \leq 1$) are the symmetric and asymmetric broadening parameters of the complex dielectric function. The contribution of dc conductivity to ε'' is due to the term $\sigma_{dc}/\varepsilon_0\omega$. The relaxation frequency, f_R , of the relaxation process is

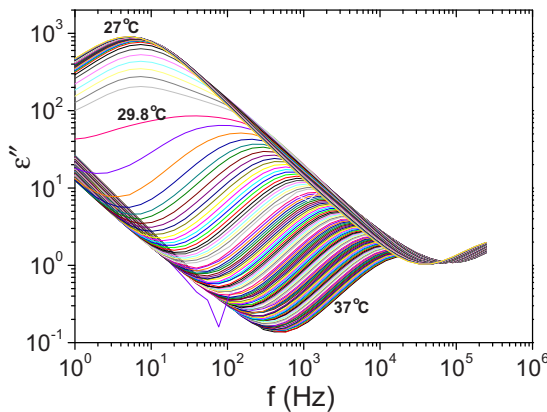


FIG. 12. Two-dimensional dielectric loss spectra as a function of frequency and temperature for a homogeneously aligned 7 μm cell of W599. The dominant ITO peak is encompassing the ε'' spectra for frequencies higher than 30 kHz.

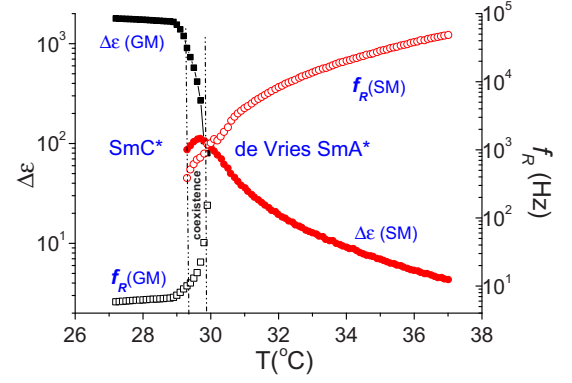


FIG. 13. Plots of the relaxation frequency (f_R) and the dielectric relaxation strength ($\Delta\varepsilon$) with temperature for W599 in a homogeneous planar-aligned 7 μm thick cell. GM and SM denote Goldstone and soft modes, respectively.

related to its relaxation time τ as [38]

$$f_R = \frac{1}{2\pi\tau} \left[\sin\left(\frac{\alpha\pi}{2+2\beta}\right) \right]^{1/\alpha} \left[\sin\left(\frac{\alpha\beta\pi}{2+2\beta}\right) \right]^{-1/\alpha}. \quad (10)$$

Figure 13 shows a strong variation in the dielectric parameters $\Delta\varepsilon$ and f_R in the Sm-A* phase. The relaxation strength increases continuously in the Sm-A* phase and reaches a maximum as the temperature tends to approach in Sm-C* is Sm-C* transition. The dielectric relaxation strength is large and is of the order of 10^3 . Such large values were previously reported by some authors [39,40]. Also, the decrement in the relaxation frequency is incessant over a broad temperature range in the Sm-A* phase. This result is in stark contrast to the trend exhibited by the conventional Sm-A* phase where sudden jumps in values of the relaxation frequency and the dielectric strength are observed close to the transition temperature [41]. The soft mode fluctuations are also very strong and consequently the dielectric absorption in Sm-A* is significantly large-another definite signature of de Vries smectics. Some of the observed features here are similar to those observed by Kocot *et al.* [42] for a siloxane polymer. This may have been the first polymeric chiral smectic studied in the literature to have de Vries characteristics.

IV. CONCLUSION

In conclusion, the two materials reported here show de Vries characteristics; these also exhibit a significantly large electroclinic effect and low orientational order parameters in their Sm-A* and Sm-C* phases. The low value of the orientational order parameter (below 0.62) as compared to conventional smectics (~ 0.8) indicates the absence of long-range correlations. The change in the dichroic ratio, the order parameter with the electric field, points towards the de Vries characteristics. The dependence of the tilt angle on the electric field can be explained by the generalized Langevin-Debye model. The results support the de Vries diffuse-cone model where the tilt angle is confined to lie within a range of values in between Ω_{\min} and Ω_{\max} , the apparent tilt angle varies with temperature/field in between these two limiting values. The change in the tilt angle with the field follows a similar trend

to what has already been observed through electro-optical experiments. The strong soft mode fluctuations in the Sm-A* are observed as evidenced by a large dielectric relaxation strength signal, which continually increases with decreasing temperature, one of the typical de Vries characteristics. The relaxation frequency softens and eventually goes towards that of the Goldstone mode in the Sm-C* phase. The two different techniques of IR and dielectric spectroscopy yield new results on the order parameter, the dichroic ratio, the relaxation strength, and the frequency of the dielectric process/es. The dependencies of these parameters on field and temperature and their interpretations in terms of models advances the understanding of de Vries smectics. These investigations rule

out the sugar-loaf model for the de Vries Smectic-A since Ω_{\min} from the birefringence measurements is much greater than zero. This is 16.9° for MSi₃MR₁₁ and 25.6° for W599.

ACKNOWLEDGMENTS

This work was supported by 13/US/I2866 from the Science Foundation of Ireland as part of the US-Ireland Research and Development Partnership program jointly administered with the United States National Science Foundation under Grant No. NSF-DMR-1410649. We thank Professor Satyendra Kumar for co-ordinating this project. Yuri P. Panarin is thanked for discussions.

- [1] S. T. Lagerwall, in *Handbook of Liquid Crystals*, edited by J. W. Goodby, P. J. Collings, T. Kato, C. Tschierske, H. F. Gleeson, and P. Raynes (Wiley-VCH, Weinheim, 2014).
- [2] P. G. de Gennes and J. Prost, *Physics of Liquid Crystals* (Clarendon Press, Oxford, 1993).
- [3] S. Garoff and R. B. Meyer, *Phys. Rev. Lett.* **38**, 848 (1977).
- [4] J. P. F. Lagerwall and F. Giesselmann, *Chem. Phys. Chem.* **7**, 20 (2006).
- [5] T. P. Rieker, N. A. Clark, G. S. Smith, D. S. Parmar, E. B. Sirota, and C. R. Safinya, *Phys. Rev. Lett.* **59**, 2658 (1987).
- [6] A. de Vries, *Mol. Cryst. Liq. Cryst.* **11**, 361 (1970).
- [7] A. de Vries, *Mol. Cryst. Liq. Cryst.* **41**, 27 (1977).
- [8] A. J. Leadbetter and E. K. Norris, *Mol. Phys.* **38**, 669 (1979).
- [9] A. de Vries, A. Ekachai, and N. Spielberg, *Mol. Cryst. Liq. Cryst.* **49**, 143 (1979).
- [10] U. Manna, J.-K. Song, Y. P. Panarin, A. Fukuda, and J. K. Vij, *Phys. Rev. E* **77**, 041707 (2008).
- [11] Y. Yamada, A. Fukuda, J. K. Vij, N. Hayashi, and T. Ando, *Liq. Cryst.* **42**, 864 (2015).
- [12] K. M. Mulligan, A. Bogner, Q. Song, C. P. J. Schubert, F. Giesselmann, and R. P. Lemieux, *J. Mater. Chem. C* **2**, 8270 (2014).
- [13] K. Merkel, A. Kocot, J. K. Vij, P. J. Stevenson, A. Panov, and D. Rodriguez, *Appl. Phys. Lett.* **108**, 243301 (2016).
- [14] S. Diele, P. Brand, and H. Sackmann, *Mol. Cryst. Liq. Cryst.* **16**, 105 (1972).
- [15] A. Gradisek, V. Domenici, T. Aphi, V. Novotna, and P. J. Sebastiao, *J. Phys. Chem. B* **120**, 4706 (2016).
- [16] K. Saunders, *Phys. Rev. E* **80**, 011703 (2009).
- [17] M. A. Osipov and M. V. Gorkunov, *Liq. Cryst.* **36**, 1281 (2009).
- [18] D. M. Agra-Kooijman, H. G. Yoon, S. Dey, and S. Kumar, *Phys. Rev. E* **89**, 032506 (2014).
- [19] G. Galli, M. Reihmann, A. Crudeli, E. Chiellini, Yu. Panarin, J. K. Vij, C. Blanc, V. Lorman, and N. Olsson, *Mol. Cryst. Liq. Cryst.* **439**, 245 (2005).
- [20] A. A. Sigarev, J. K. Vij, Y. P. Panarin, P. Rudquist, S. T. Lagerwall, and G. Heppke, *Liq. Cryst.* **30**, 149 (2003); B. K. P. Scaife and J. K. Vij, *J. Chem. Phys.* **122**, 174901 (2005).
- [21] K. Merkel, A. Kocot, J. K. Vij, G. H. Mehl, and T. Meyer, *J. Chem. Phys.* **121**, 5012 (2004).
- [22] A. Kocot and J. K. Vij, *Liq. Cryst.* **37**, 653 (2010).
- [23] A. Kocot, G. Kruk, R. Wrzalik, and J. K. Vij, *Liq. Cryst.* **12**, 1005 (1992); A. Kocot, R. Wrzalik, B. Orgasinska, T. Perova, J. K. Vij, and H. T. Nguyen, *Phys. Rev. E* **59**, 551 (1999).
- [24] A. A. Sigarev, J. K. Vij, R. A. Lewis, M. Hird, and J. W. Goodby, *Phys. Rev. E* **68**, 031707 (2003).
- [25] O. E. Kalinovskaya, Yu. P. Panarin, and J. K. Vij, *Europhys. Lett.* **57**, 184 (2002).
- [26] S. P. Sreenilayam, D. M. Agra-Kooijman, V. P. Panov, V. Swaminathan, J. K. Vij, Yu. P. Panarin, A. Kocot, A. Panov, D. Rodriguez-Lojo, P. J. Stevenson, M. R. Fisch, and S. Kumar, *Phys. Rev. E* **95**, 032701 (2017).
- [27] Y. Shen, L. Wang, R. Shao, T. Gong, C. Zhu, H. Yang, J. E. MacLennan, D. M. Walba, and N. A. Clark, *Phys. Rev. E* **88**, 062504 (2013).
- [28] S. Inui, N. Iimura, T. Suzuki, H. Iwane, K. Miyachi, Y. Takanishi, and A. Fukuda, *J. Mater. Chem.* **6**, 671 (1996).
- [29] N. A. Clark, T. Bellini, R.-F. Shao, D. Coleman, S. Bardon, D. R. Link, J. E. MacLennan, X.-H. Chen, M. D. Wand, D. M. Walba, P. Rudquist, and S. T. Lagerwall, *Appl. Phys. Lett.* **80**, 4097 (2002).
- [30] J. V. Selinger, P. J. Collings, and R. Shashidhar, *Phys. Rev. E* **64**, 061705 (2001).
- [31] Z. V. Kost-Smith, P. D. Beale, N. A. Clark, and M. A. Glaser, *Phys. Rev. E* **87**, 050502(R) (2013).
- [32] K. Zappitelli, D. N. Hipolite, and K. Saunders, *Phys. Rev. E* **89**, 022502 (2014); K. Saunders, *ibid.* **77**, 061708 (2008).
- [33] P. J. Collings, B. R. Ratna, and R. Shashidhar, *Phys. Rev. E* **67**, 021705 (2003).
- [34] N. Hayashi, T. Kato, A. Fukuda, J. K. Vij, Y. P. Panarin, J. Naciri, R. Shashidhar, S. Kawada, and S. Kondoh, *Phys. Rev. E* **71**, 041705 (2005).
- [35] K. L. Sandhya, Y. P. Panarin, V. P. Panov, J. K. Vij, and R. Dabrowski, *Eur. Phys. J. E* **27**, 397 (2008).
- [36] O. E. Panarina, Y. P. Panarin, J. K. Vij, M. S. Spector, and R. Shashidhar, *Phys. Rev. E* **67**, 051709 (2003).
- [37] M. R. Dodge, J. K. Vij, S. J. Cowling, A. W. Hall, and J. W. Goodby, *Liq. Cryst.* **32**, 1045 (2005).
- [38] O. E. Kalinovskaya and J. K. Vij, *J. Chem. Phys.* **111**, 10979 (1999).
- [39] F. Gouda, K. Skarp, and S. T. Lagerwall, *Ferroelectrics* **113**, 165 (1991).
- [40] U. Manna, J.-K. Song, J. K. Vij, and J. Naciri, *Phys. Rev. E* **78**, 041705 (2008).
- [41] H. Xu, J. K. Vij, A. Rappaport, and N. A. Clark, *Phys. Rev. Lett.* **79**, 249 (1997).
- [42] A. Kocot, R. Wrzalik, J. K. Vij, M. Brehmer, and R. Zentel, *Phys. Rev. B* **50**, 16346 (1994).